MHD Dynamo Simulation Using GeoFEM Platform

Hiroaki MATSUI

Department of Research for Computational Earth Science, Research Organization for Information Science & Technology (RIST), 2-2-54, Naka-meguro, Meguro-ku, Tokyo 153-0061, JAPAN, matsui@tokyo.rist.or.jp

Introduction

It has been widely accepted that the geomagnetic field is generated by motion of an electrically conducting fluid in the Earth's outer core. This process is referred to as geodynamo. Numerical simulation has played a large role in understanding the geodynamo process. Most of these simulations utilized the spherical harmonics expansion (Glatzmaier and Roberts, 1995[1]; Kuang and Bloxham, 1999[2]). However, this scheme is not suitable for massively parallel computation because a significant number of global calculations are required. We have been developing a simulation code for the MHD simulation of a fluid in a rotating spherical shell using GeoFEM, which provides a parallel finite-element method (FEM) platform for solid Earth simulation. The most difficult problem for the geodynamo simulation using FEM is to solve the magnetic field at boundaries of the fluid shell: That is, the magnetic field in the fluid shell is connected to a potential field in outside of the shell and the potential field is solved simultaneously. A finite element mesh was not only set for the fluid shell but for the outside of the fluid shell to solve the magnetic field in the insulated area. A radius of the finite element mesh is set to be approximately 15 times of the width of the fluid shell and boundary condition are set at outside of the mesh instead of the magnetic boundary condition for the infinite radius. Furthermore, the vector potential of the magnetic field is chosen for the time evolution of the magnetic field to satisfy the boundary condition at the boundaries of the fluid shell. To verify the simulation code, a MHD simulation is performed with same geometry and dimensionless numbers using FEM and using spherical harmonics expansion. These results show that outlines of convection and magnetic field patterns are similar to each other. However, intensity of the average magnetic energy in the FEM case is approximately 90 % of that in the case of the spherical harmonics expansion, while intensity of the kinetic energy is almost same in the two cases.

Simulation Model and Methods

Models

Consider a rotating spherical shell modeled on the Earth's outer core. The ratio of the inner boundary to outer boundary of the spherical shell is set to 0.4 while the ratio of the radius of the inner core boundary (ICB) to that of the core-mantle boundary (CMB) is approximately 0.35. The radii of the inner boundary and the

outer boundary of the fluid shell are set to be $r_i = 2/3$ and $r_o = 5/3$, respectively. The shell is filled with an electrically conductive fluid and rotates with a constant angular velocity Ω. The fluid has a constant thermal diffusivity κ, kinetic diffusivity ν, magnetic diffusivity η, and thermal expansion coefficient α. We assume that the inner core is electrically insulated and that co-rotates with the mantle to compare with a simulation using a spherical harmonics expansion. In the present simulation, a momentum equation with buoyancy, Coriolis, and Lorentz terms, the heat conduction equation, the magnetic induction equation, and the conservation laws for the incompressible fluid and the magnetic field are solved. Normalized basic equations for the fluid motion and temperature are given the following;

$$\begin{aligned}
\frac{\partial \boldsymbol{u}}{\partial t} + (\boldsymbol{u}\cdot\nabla)\,\boldsymbol{u} &= -\nabla\chi + P_r\nabla^2\boldsymbol{u} - P_r\sqrt{T_a}\,(\boldsymbol{\Omega}\times\boldsymbol{u}) \\
&\quad + P_r R_a\,(T - T_0)\,\boldsymbol{r} + P_r\,(\nabla\times\boldsymbol{B})\times\boldsymbol{B}, \qquad (1)\\
\frac{\partial T}{\partial t} + (\boldsymbol{u}\cdot\nabla)\,T &= \nabla^2 T, \text{ and} \qquad (2)\\
\operatorname{div}\boldsymbol{u} &= 0, \qquad (3)
\end{aligned}$$

where, χ and T_0 are described with perturbation of the pressure from a hydrostatic state P, magnetic field B, and radius r as following;

$$\begin{aligned}
\chi &= P + \frac{1}{2}P_r B^2, \text{ and} \qquad (4)\\
T_0 &= \frac{r_i r_o - r_i r}{r\,(r_o - r_i)}. \qquad (5)
\end{aligned}$$

For the magnetic field in the conductive fluid, the following equations are solved;

$$\begin{aligned}
\frac{\partial \boldsymbol{A}}{\partial t} &= -\nabla\varphi + \frac{P_r}{P_m}\nabla^2\boldsymbol{A} + \boldsymbol{u}\times\boldsymbol{B}, \qquad (6)\\
\operatorname{div}\boldsymbol{A} &= 0, \text{ and} \qquad (7)\\
\boldsymbol{B} &= \nabla\times\boldsymbol{A}, \qquad (8)
\end{aligned}$$

where, $\boldsymbol{A}$ is the vector potential of the magnetic field. Furthermore, the magnetic field in the outside of the core is solved by the following equations;

$$\begin{aligned}
0 &= \frac{P_r}{P_m}\nabla^2\boldsymbol{A}, \text{ and} \qquad (9)\\
\nabla\cdot\boldsymbol{A} &= 0.
\end{aligned}$$

Four dimensionless numbers appear in the basic equations; that is, the Prandtl number P_r, the magnetic Prandtl number P_m, the Taylor number T_a, and the Rayleigh number R_a are defined by,

$$\begin{aligned}
P_r &= \frac{\nu}{\kappa}, \qquad (10)\\
P_m &= \frac{\nu}{\eta}, \qquad (11)\\
T_a &= \left(\frac{2\Omega L^2}{\nu}\right)^2, \text{ and} \qquad (12)\\
R_a &= \frac{\alpha g \Delta T L^3}{\kappa\nu}, \qquad (13)
\end{aligned}$$

where, g is a magnitude of gravity on the core-mantle boundary. The Taylor number and Rayleigh number in the Earth's core are estimated to be $T_a = 10^{30}$ and $R_a = 6 \times 10^{30}$ with molecular viscosities. Even if we consider turbulent viscosities, these dimensionless numbers remain much greater than 10^{10}. However, these estimated values can not be used directly because of limitation of computational power. Therefore, let the Prandtl number be 1, the Taylor number be 9.0×10^4, the Rayleigh number be 1.2×10^4, and the magnetic Prandtl number be 10.0.

Simulation Methods and Finite Element Mesh

All physical values (velocity $\boldsymbol{u}$, temperature T, the vector potential of the magnetic field $\boldsymbol{A}$, and potential φ) are interpolated by tri-linear function in each hexahedral element. A fractional step scheme is applied for integration over time. To obtain the magnetic field in the fluid shell and in outside of the shell. To solve eqs. (6) and (9) simultaneously, the diffusion terms are solved by the Crank-Nicolson scheme and the other terms are solved by the Adams-Bashforth scheme in the time evolution processes. Because characteristics of the convection pattern are that thin boundary layer will be generated around the boundaries of the shell, it is possible to apply longer length of time step in this scheme that in explicit schemes. The pressure and the scalar potential are solved by their Poisson equations to satisfy the conservation laws. Parallel CG solver is chosen to solve the diffusion terms and the Poisson equations. A finite element mesh is considered only for the northern hemisphere to reduce the number of elements, and the velocity, temperature, pressure, and vector potential are assumed to be symmetric with respect to the equatorial plane. As

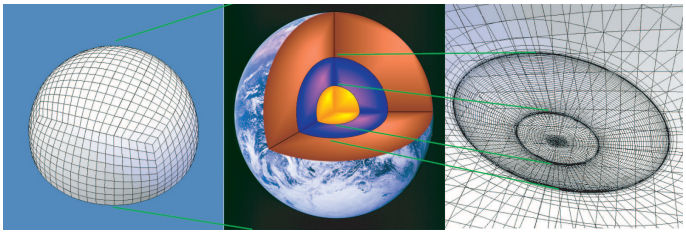

Figure 1: Finite element mesh (left and right panels) and sketch of the interior of the Earth (middle panel). The entire mesh patterns is given in the left, and the detailed mesh pattern to see the fluid shell is given in the right.

seen in Fig. 1, the grid pattern is based on the cubic pattern; that is, a cubic pattern is projected to a sphere surface and stacked into the radial direction. To solve the potential field external to the fluid shell, the finite element mesh is set to $r_{max} = 14.8L = 5.09R_e$, where R_e is the radius of the Earth. The mesh has 77760 elements, and nodes 46656 elements are for the fluid shell.

Boundary conditions are important for this study. We apply the non-slip boundary condition for the velocity field on the boundaries of the shell, and set the temperature to be 1 on the inner boundary of the fluid shell and 0 on the outer boundary of the fluid shell. The vector potential is set to be 0 on the outer boundary of the finite element mesh instead of the boundary condition at infinite radius. To consider the symmetry with respect to the equatorial plane, the following conditions are set

at the equatorial plane;

$$\frac{\partial u_x}{\partial z} = \frac{\partial u_y}{\partial z} = u_z = 0, \tag{14}$$

$$\frac{\partial T}{\partial z} = 0, \tag{15}$$

$$\frac{\partial A_x}{\partial z} = \frac{\partial A_y}{\partial z} = A_z = 0, \text{ and} \tag{16}$$

$$B_x = B_y = \frac{\partial B_z}{\partial z} = 0. \tag{17}$$

The present simulation was performed on 4 nodes of SR8000 which has 8 processors in each node. OpenMP is used for parallelization of intra-node, and MPI is used for communication among nodes. Because domain decomposition is used for the inter node parallelization, the finite element mesh is divided into 4 sub-domains.

Simulation by the spectral method

To verify the results of the simulation by GeoFEM, the same simulation was carried out by the spectral method. In this case, the simulation scheme is based on those of Frazer [3], Honkura et. al. [4], and Matsui [5]. Scalar functions of the poloidal and toroidal components of the velocity and magnetic fields, and temperature perturbation are expanded in spherical harmonics. To find a solution in the radial direction, the second-order FDM is applied. The vorticity equation and the heat conduction equation, and the magnetic induction equation are solved in this case. To solve the time evolution, the Crank-Nicolson scheme is adopted for the diffusion terms and the second-order Adams-Bashforth scheme used for solving the remaining terms. It is noted that the advection terms, the Coriolis term, and the Lorentz term, and the induction term are solved by the coefficients of the spherical harmonics. Because the amount of the computation increased by $O(L^5)$ in this scheme, it is difficult to set the truncation levels to be significantly large. The truncation level of the spherical harmonics is set to be 18 degrees with 64 equality spaced grid points in the radial direction in this study. The simulation was performed on 32 processors of NEC SX-4.

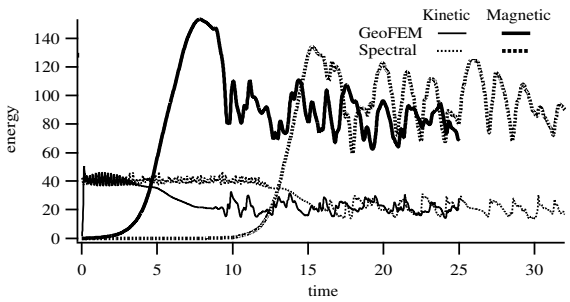

Figure 2: Time evolution of the kinetic and magnetic energy averaged over the fluid shell. Results by FEM are given by solid lines, and results by spectral method are given by dotted lines. The kinetic and magnetic energies are shown by thin lines and thick lines, respectively.

Results

Time evolutions of kinetic and magnetic energies averaged over the fluid shell are given in Fig. 2. The simulation results show that the magnetic energy in the fluid shell reaches approximately 4 times of the kinetic energy. Comparing with results in the case of the spectral method, magnitude of the magnetic energy in the case of FEM is approximately 90% of that in the case of spectral method while magnitude of the kinetic energy is almost same in these cases. This difference is caused by difference of the spatial resolution between the two cases. The convection and magnetic field patterns in these cases are given Fig. 3. As seen in this figure, z-component of the

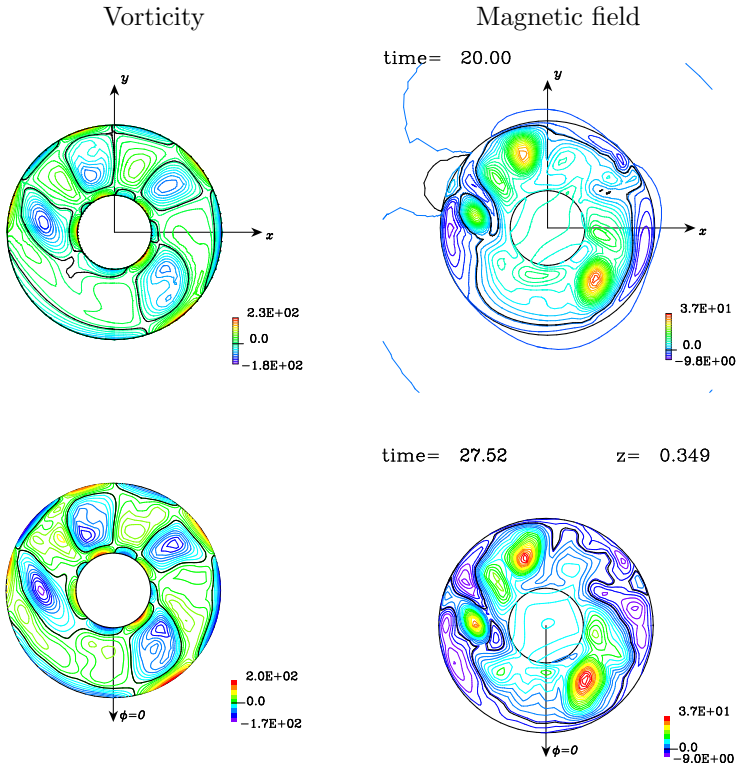

Figure 3: Intensity of the z-component of the vorticity (left panels) and intensity of the z-component of the magnetic field (right panels) in a cross section at $z = 0.35$. Results by FEM case for $t = 20.0$ are given in upper panels, and results in the case of spectral method for $t = 27.52$ are given in lower panels.

magnetic field is strongly generated in the convection columns which have negative z-component of the vorticity while the flow pattern is disturbed by the Lorentz force in both cases. The characteristics of the velocity and magnetic fields are common with that observed in previous spectral MHD simulations. Some differences can be seen between the two results in detail; that is, small scale structures are shown in the

case of spectral method. Because the truncation level is only 18 degree, this small scale magnetic field is intensified by the artificial truncation. However, we consider that the spatial resolution is still small in the GeoFEM case and that the small scale magnetic fields are not represented correctly in GeoFEM case.

Conclusion

A magnetohydrodynamic (MHD) simulation of the fluid motion in a rotating spherical shell modeled on the Earth's outer core was performed using the finite element method (FEM). The simulation is for understanding of the origin of the geomagnetic field and for understanding of the dynamics of the fluid in the Earth's outer core. To verify the present simulation code, the simulation results were compared with that by spectral harmonics expansion. These results show that outlines of the convection and magnetic field patterns have same characteristics while average magnetic energy is approximately 90 % of that in the case of spherical harmonics expansion. However, outlines of the convection and magnetic field patterns are similar to each other. For more verification of the present simulation code, we will test the simulation code with a numerical dynamo benchmark test by Christensen et. al.(2001)[6]. For understanding of the geodynamo processes, we will perform the simulation with rapid rotation and strong buoyancy. Because much higher spatial resolution is required in the simulation, the simulation will be performed on the Earth Simulator which has 640 nodes with SMP type 8 vector processors.

References

[1] Glatzmaier, G. A. and Roberts, P. H., A three-dimensional convective dynamo solution with rotating and finitely conducting inner core and mantle, *Phys. Earth Planet. Inter.* , **91**, 63-75, 1995.

[2] Kuang, W. and Bloxham, J., Numerical modeling of magnetohydrodynamics convection in a rapidly rotating spherical shell: weak and strong field dynamo action, *J. Comput. Phys.* , **153**, 51-81, 1999.

[3] Frazer, M.C., Spherical hermonic analysis of the Navier-Stokes equation in magnetofluid dynamics, *Physics of Earth and Planetary Interiors*, **8**, 75-82,1974.

[4] Honkura, Y., T.Iijima and M. Matsushima, Magnetic field reversal resulting from a dynamo process in a spherical shell, *Journal of Geomagnetism and Geoelectricity*, **2**, 1421-1431, 1995.

[5] Hiroaki Matsui, Studies on the Basic Processes of Magnetic Field Generation Based on MHD Simulation in the Rotating Spherical Shell, Ph.D. Thesis, Tohoku Univ.,1999.

[6] Christensen, U. R., Aubert, J., Cardin, P., Dormy, E., Gibbons, S., Glatzmaier, G. A., Grote, E., Honkura, H., Jones, C., Kono, M., Matsushima, M., Sakuraba, A., Takahashi, F., Tilinger, A., Wicht, J., and Zhang, K., A numerical dynamo benchmark, *Phys. Earth Planet. Inter.* , **128**, 25-34, 2001.